Characterizing Cardiac Adipose Tissue in Post-AMI Patients via CT Imaging: A Comparative Cross-sectional Study

Mr. Xiaomeng Wang [1], Dr. Shuang Leng [2,3], Prof. Philip D Adamson [4,5], Dr. Charlotte E Greer [4], Dr. Weimin Huang [6], Dr. Hwee Kuan Lee [7], Ms. Yan Ting Loong [2], Ms. Nur Amirah Syahindah Raffiee [2], Dr. Ching Hui Sia [8,9], Dr. Swee Yaw Tan [1,2], Dr. Sock Hwee Tan [9], Dr. Lynette Li San Teo [10], Dr. Sung Lung Wong [2], Ms. Xiaoxun Yang [9], Dr. Min Sen Yew MBBS[11], Dr. Thon Hon Yong MBChB[12], Prof. Liang Zhong [1,2,14,17,18], Prof. Leslee J Shaw [13], Prof. Mark Yan Yee Chan [8,9], Prof. Derek J Hausenloy [1,14,15,16*], Dr. Lohendran Baskaran [2,14,3,17*]

[*]These authors are joint senior

[1]Cardiovascular and Metabolic Disorders Programme, Duke-National University of Singapore, Singapore, Singapore,

[2]National Heart Center Singapore, Singapore, Singapore,

[3]Duke-National University of Singapore, Singapore, Singapore,

[4]Department of Medicine, University of Otago Christchurch, Christchurch, New Zealand,

[5]BHF Centre for Cardiovascular Science, University of Edinburgh, Edinburgh, UK,

[6]Institute for Infocomm Research, Agency for Science, Technology and Research (A*Star), Singapore, Singapore,

[7]Bioinformatics Institute, Agency for Science, Technology and Research (A*Star), Singapore, Singapore,

[8]National University Heart Center Singapore, Singapore, Singapore,

[9]Yong Loo Lin School of Medicine, National University of Singapore, Singapore, Singapore,

[10]Department of Diagnostic Imaging, National University Hospital, Singapore, Singapore,
[11]Department of Cardiology, Tan Tock Seng Hospital, Singapore, Singapore,
[12]Department of Cardiology, Changi General Hospital, Singapore, Singapore,
[13]Icahn School of Medicine at Mount Sinai, New York City, NY, US,
[14]National Heart Research Institute Singapore, National Heart Centre, Singapore, Singapore,
[15]Yong Loo Lin School of Medicine, National University Singapore, Singapore, Singapore,
[16]The Hatter Cardiovascular Institute, University College London, London, UK,
[17]CVS.AI, National Heart Research Institute Singapore, National Heart Centre, Singapore, Singapore
[18]Department of Biomedical Engineering, National University of Singapore

*** Corresponding author:**
Clin Asst Prof Lohendran Baskaran,
Department of Cardiology,
National Heart Centre Singapore,
5 Hospital Drive, Singapore 169609.
E-mail: lohendran_baskaran@duke-nus.edu.sg

Abstract

Aims: To identify differences in CT-derived perivascular (PVAT) and epicardial adipose tissue (EAT) characteristics that may indicate inflammatory status differences between post-treatment acute myocardial infarction (AMI) and stable coronary artery disease (CAD) patients.

Methods and Results: A cohort of 205 post-AMI patients (age 59.8±9.2, 92.2% male) was propensity-matched with 205 stable CAD patients (age 60.5±10.0, 90.2% male). Coronary CT angiography and non-contrast CT scans were performed to assess PVAT mean attenuation across major coronary segments and EAT mean attenuation and volumes, respectively. For post-AMI patients, CT scans were conducted 28.6 ± 13.8 days after the AMI incidence. Post-AMI patients showed higher non-culprit PVAT and EAT mean attenuation than stable CAD patients (8.01HU, 95% CI 5.90 to 10.11 HU, p<0.001, 2.48 HU, 95% CI 0.83 to 4.13 HU, p=0.003, respectively). The EAT volume percentage at higher attenuation levels was higher in post-AMI patients compared to stable CAD (33.93cm^3, 95% CI 16.86 to 51.00 cm^3, p<0.001), with the difference maximized at the -70 HU threshold (4.75%, 95% CI 3.64% to 5.87%, p<0.001). PVAT mean attenuation positively correlated with EAT mean attenuations and the percentage of EAT volume >-70 HU (p<0.001 for both).

Conclusions: Post-AMI patients showed higher PVAT and EAT attenuation than stable CAD patients, potentially indicating AMI-associated inflammatory cardiac adipose tissue changes. -70 HU can act as a potential cut-off for inflamed EAT. These findings highlight the potential of using CT-derived adipose tissue characteristics to assess inflammation and guide post-AMI management strategies.

Keywords: Acute myocardial infarction, computed tomography, perivascular adipose tissue, epicardial adipose tissue

Introduction

Coronary artery disease (CAD) and acute myocardial infarction (AMI) are manifestations of the atherosclerotic process, an inflammatory disease of the blood vessels by the core (1). Despite a common pathological source, CAD may unfold as a chronic condition, with clinically silent periods occasionally interspersed with episodes of stable angina, whereas AMI is acute and often severe (2, 3).

Instead of being mere fat reservoirs, perivascular adipose tissue (PVAT) and epicardial adipose tissue (EAT) appear to be active paracrine entities capable of secreting a range of inflammatory mediators. PVAT surrounds the coronary vessels and can promote vascular inflammation by releasing pro-inflammatory cytokines, which influence adjacent vascular cells (4). Similarly, EAT, located between the myocardium and visceral pericardium, may directly impact myocardial and coronary vessel function by secretion of bioactive molecules (5). These locally acting mediators can modulate vascular health, potentially amplifying the progression of atherosclerosis and its complications (4-6). Advancements in imaging techniques now allow the exploration of these tissues as potential inflammatory biomarkers in cardiovascular patients (5, 7, 8).

However, significant knowledge gaps remain in the study of PVAT and EAT as indicators of inflammation. No studies have investigated how EAT characteristics differ between recent AMI patients with heightened inflammation and stable CAD patients with subdued inflammation (5, 9, 10). Furthermore, much of the extant research focuses on the primary lesions and vessels in AMI cases. Non-culprit regions, which could provide a broader perspective on post-treatment inflammation, have not been as extensively studied (11). Additionally, the relationship between PVAT and EAT has not been thoroughly investigated, limiting a comprehensive understanding of cardiac inflammation (12, 13).

This study aims to identify changes in post-AMI PVAT and EAT characteristics that may indicate residual inflammatory risk. Using coronary computed tomography angiography (CCTA) for PVAT and non-contrast computed tomography (NCCT) for EAT, respectively, we compared recent AMI patients to those with stable CAD. We hypothesize that individuals recovering from a recent AMI will exhibit more pronounced inflammation-associated PVAT and EAT characteristics than those with stable CAD. We further evaluated the relationship between PVAT and EAT characteristics.

Materials and Methods

Study Design and Study Population

This cross-sectional analysis included 205 post-AMI patients recruited from eight Singapore and New Zealand hospitals (**Supplementary Method**) from 2021 to 2023. All post-AMI patients underwent CCTA ≤ 2 months post-AMI incidence (**Figure 1**). AMI was defined by the universal definition (14). This study was approved by each site's Institutional Review Board. Clinical research coordinators at each site collected patient demographic and clinical information during recruitment. Among these 205 patients, 129 patients also received concurrent non-contrast CT (NCCT) scans. These recent AMI patients were 1:1 propensity-matched to stable CAD patients, defined as CAD patients with no history of cardiac events or procedures, via the nearest neighboring approach (15). The stable CAD patients were identified from the image database of APOLLO (AI-driven national platform for CT coronary angiography for clinical and industrial applications, clinicaltrials.gov identifier NCT05509010) registry, where 1200 cases with suspected or known CAD who had undergone both CCTA and NCCT between 2007 and 2017 in three Singapore hospitals (**Supplementary Method**) and had no cardiac event or coronary revascularization (percutaneous coronary intervention [PCI] and coronary artery bypass grafting [CABG]) before scans. Each site obtained approval from the local institutional review board or ethics board and submitted de-identified scans for analysis.

Consents

Written consents were obtained from all participants.

Cardiac CT Acquisition

CCTA and gated NCCT were performed using computed tomography scanners of ≥ 256-detector rows under each site's resident CT imaging protocol, in line with Society of Cardiovascular Computed Tomography (SCCT) guidelines (CCTA: contrast dosage 72.45 ± 23.20 mL, 355 patients [86.59%] underwent prospective gating, tube voltage 110 - 120 kVp, tube current 175.80 ± 138.66 mAs, dose length product 203.82 ± 176.84 mGy*cm; NCCT: tube voltage 120 kVp, tube current 312.05 ± 140.14 mA, dose length product 58.25 ± 52.19 mGy*cm) (16, 17). Site-submitted Digital Imaging and Communications in Medicine files masked to clinical results and case status were analyzed in the CardioVascular Systems Imaging and Artificial Intelligence (CVS.AI) research core in the National Heart Center Singapore.

CCTA Analysis

Three independent readers with >3 years of experience at the CVS.AI research core performed standardized measurements using semi-automated analysis software (QAngioCT Research Edition version 3.2.0.13, Medis, Leiden) with appropriate manual correction (18).

PVAT mean attenuation was measured in four major coronary vessel segments (left main [LM], proximal left anterior descending [pLAD], proximal left circumflex [pLCX], and proximal right coronary artery [pRCA]), excluding culprit vessels containing PCI stents in post-AMI patients (19-21). For each segment, PVAT was defined as voxels located within the radial distance from the vessel wall equal in thickness to the average diameter of the segment (**Figure 2**) (7, 19-22). In this region, PVAT mean attenuation was then calculated as the average attenuation of all PVAT

voxels. A per-patient pooled PVAT mean attenuation was also derived by averaging PVAT mean attenuation from all four segments. The interobserver and intraobserver intraclass correlation coefficients (ICC) for pooled PVAT mean attenuation were 0.991 and 0.996, and the coefficients of variation (CV) were 1.25% and 0.67%, respectively (**Supplementary Method**).

NCCT Analysis

Three independent readers with >3 years of experience at the CVS.AI research core manually segmented the pericardium using open-source software with established procedures (3D Slicer, Boston, MA) (23, 24). EAT region was automatically segmented in the pericardium with an attenuation threshold of -190 – -30 HU. EAT characteristics were quantified using custom MATLAB programs (MATLAB 2022a, Mathworks, Natick, MA). In this study, we evaluated EAT mean attenuation, EAT volume, and the percentage of EAT volume exceeding predefined HU thresholds. For the latter, we determined the percentage of EAT voxels with an HU value greater than designated thresholds, ranging between -80 and -60 HU, based on previous literature (10). The interobserver and intraobserver ICC for EAT volume were 0.992 and 0.995, and the CVs were 5.26% and 2.19%, respectively (**Supplementary Method**).

Statistical Analysis

At the patient level, post-AMI patients were compared to matched stable CAD patients. Continuous variables are expressed as mean ± standard deviation (SD), and categorical variables are presented as absolute counts and percentages. Differences between categorical variables were analyzed using Fisher's exact or chi-square test, as appropriate, and those between continuous variables using student's t-test. Univariate linear correlations between continuous variables were examined using Pearson's correlation coefficient.

Multivariate linear regression models were used to compare EAT characteristics and PVAT mean attenuation differences between propensity-matched post-AMI and stable CAD cohorts at the per-patient level and to extrapolate the correlation between PVAT mean attenuation and EAT characteristics. Models were adjusted for age, sex, race, smoking history, hypertension, DM, hyperlipidemia, body mass indexes (BMI), family history of CAD, use of lipid control medications, and tube voltage due to their established contribution to CAD risks and CT scan results (20, 25). Models were also adjusted for EAT volume for EAT attenuation comparison and lumen attenuation for PVAT comparison (20). For the comparison of pooled PVAT mean attenuation, the regression model was further adjusted for the location of vessel segments. Coefficients of the fitted linear model were expressed as expected value ± standard error (SE). Estimated statistics from fitted models, averaging all covariates, were calculated with the margins function of STATA.

A 2-tailed p-value <0.05 was considered to indicate a statistically significant difference. All analyses were performed with STATA version 17.0 (StataCorp, College Station, TX) and R version 4.1.2 (R Foundation for Statistical Computing, Vienna). Sensitivity analyses for races and BMI were performed to assess the robustness of our findings.

Results

Patient Characteristics

The final study cohort comprised 205 post-AMI cases and 205 propensity-matched stable CAD subjects with CVS.AI research core-measured CCTA. Post-AMI patients received cardiac CT scans 28.6 ± 13.8 days after the AMI incidence. 291 stent-containing vessels were excluded, including 205 culprit and 86 non-culprit vessels (**Table S1**). Within the study cohort, 129 post-AMI cases and 129 propensity-matched stable CAD subjects were with CVS.AI research core-measured NCCT. The average age of the post-AMI cohort was 59.8 ± 9.2 years (92.2% male; 45.9% Chinese, 14.2% Indian, 8.8% Malay, 26.3% Caucasian, 4.9% other or unknown race), and

the average age of the stable CAD cohort was 60.5 ± 10.0 years (90.2% male; 76.6% Chinese, 9.3% Indian, 3.9% Malay, 1.0% Caucasian, 9.3% other or unknown race) (**Table 1**). Post-AMI (62.4% ST-elevation myocardial infarction [STEMI], 37.6% non-STEMI) and stable CAD patients were well matched by propensity score (0.426 ± 0.182 vs. 0.396 ± 0.182; p = 0.105) (**Table 1**). Propensity-score-matched post-AMI and stable CAD patients had similar risk factors (hypertension, hyperlipidemia, DM, family history of premature CAD, and smoking status), but post-AMI cases had higher BMI (27.3 ± 4.5 vs. 25.8 ± 5.2, p = 0.001), which was not a component of the propensity score (**Table 1**).

PVAT Analysis

In univariate analysis, post-AMI patients demonstrated higher pooled PVAT mean attenuation (-73.25 ± 9.2 HU vs. -78.82 ± 9.2 HU) and higher attenuation in each major segment (p < 0.05 for all), except pRCA (-75.6 ± 8.3 HU vs. -76.7 ± 7.6 HU, p = 0.241), compared to stable CAD patients (**Table S2**). In multivariate analysis, post-AMI patients were observed to have a significantly higher pooled PVAT mean attenuation than stable CAD patients by 8.01 HU (estimate = 8.01, 95% CI = [5.90, 10.11], p < 0.001) (**Table 2**, **Figure 3a**). Among these four segments, post-AMI patients exhibited significantly higher PVAT mean attenuation than stable CAD patients in all four coronary vessel segments (LM estimate = estimate = 11.5, 95% CI = [8.59, 14.41], p < 0.001, pLAD estimate = 6.45, 95% CI = [3.02, 9.89], p < 0.001, pLCX estimate = 6.93, 95% CI = [4.22, 9.63], p < 0.001, pRCA estimate = 4.62, 95% CI = [1.76, 7.48], p = 0.002) (**Table 2**, **Figure 3b – e**).

EAT Analysis

In univariate analysis, post-AMI patients exhibited a higher EAT mean attenuation (-74.3 ± 4.8 HU vs. -76.9 ± 5.4 HU, p < 0.05) and volume (147.97 ± 51.66 cm^3 vs. 129.29 ± 48.42 cm^3, p < 0.05) than stable CAD patients (**Table S2**). In multivariate analysis, males had higher EAT mean

attenuation than females by 3.36 HU (estimate = 3.36, 95% CI = [1.68, 5.05], p < 0.001), while an increase in age of one year was associated with a rise of 1.06 cm^3 in EAT volume (estimate = 1.06, 95% CI = [0.35, 1.78], p = 0.004). Upon adjustment, post-AMI patients displayed significantly elevated EAT mean attenuation compared to stable CAD patients by 2.48 HU (estimate = 2.48, 95% CI = [0.83, 4.13], p = 0.003) and EAT volume by 33.93 cm^3 (estimate = 33.93, 95% CI = [16.86, 51.00], p < 0.001) (**Table 2**, **Figure 4**).

In the multivariable comparison of the percentage of EAT volume above specified attenuation thresholds, set from -80 to -60 HU, percentages of EAT volume were consistently higher for post-AMI patients (p < 0.05 for all). The differences in EAT volume percentages peaked at a threshold of -70 HU, with a difference of 4.75% (estimate = 4.75, 95% CI = [3.64, 5.87], p < 0.001), thus justifying the selection of -70 HU as the threshold indicative of inflamed EAT (**Figure S1**).

In the multivariable correlation analysis between PVAT mean attenuation and EAT characteristics, a rise in pooled PVAT mean attenuation corresponded with an increase in both EAT mean attenuation (estimate = 0.204, 95% CI = [0.129, 0.279], p < 0.001) and percentage of EAT volume percentage > -70 HU (estimate = 0.407, 95% CI = [0.302, 0.513], p < 0.001) (**Figure S2ac, Table S3**). Conversely, an increase in pooled PVAT mean attenuation was linked to a reduction in EAT volume (estimate = -2.615, 95% CI = [-3.25, -1.981], p < 0.001) (**Figure S2b, Table S3**). These patterns persisted across all four vessel segments (p < 0.05 for all) (**Table S3**) and in the sub-cohort analysis within the post-AMI and stable CAD cohorts (**Table S4**).

Sensitivity Analysis

To address the potential confounding effects of BMI, hyperlipidemia, and race, we conducted two sensitivity analyses **(Supplementary Result)**. First, in a BMI-hyperlipidemia-matched cohort, we found that the primary findings remained consistent, with post-AMI patients exhibiting significantly

higher PVAT and EAT mean attenuation, increased EAT volume, and a higher percentage of EAT volume > -70 HU. Second, in a subgroup analysis restricted to Chinese patients, similar trends were observed. These analyses confirm that our main findings are robust across variations in BMI and racial background.

Discussion

This study compared CCTA-derived PVAT and NCCT-derived EAT characteristics in stable CAD and post-AMI patients from a multiethnic Asian-Pacific cohort. We found that, compared to stable CAD patients, post-AMI is associated with higher PVAT mean attenuation, EAT volumes, and EAT mean attenuation, which positively correlated to PVAT mean attenuation. These observations could be associated with residual inflammatory risk in post-AMI patients. Finally, this study identifies a -70 HU threshold of EAT volume as a potential measurable indicator for assessing cardiac inflammation. This research is among the initial efforts to thoroughly compare CT-derived PVAT and EAT in stable CAD and post-AMI patients.

There was a significant increase in PVAT mean attenuation in non-culprit vessels of post-AMI patients. Previous studies have associated increased PVAT attenuation with vascular inflammation, plaque progression, and adverse cardiovascular events (4, 6-8, 19, 20). It is theorized that localized "cachexia-type" response in PVAT adjacent to inflamed vessel walls can lead to smaller, less lipid-rich adipocytes and increased CT attenuation at the macroscopic level (4). Thus, our results of increased PVAT attenuation in post-AMI patients may indicate a continued vascular inflammatory response after AMI.

Unique to our study is the evaluation of EAT in post-AMI patients, where we observed higher EAT volume and mean attenuation compared to stable CAD patients. EAT volume has been

established as a predictor for obstructive CAD, major adverse cardiovascular events, coronary calcium score (CAC), and vulnerable coronary plaques (5, 26-28). Prior research has also linked increased EAT attenuation to a higher CAC, an increased risk of CAD and AMI, and other inflammatory conditions (e.g., severe COVID-19) (28-31). Meanwhile, some studies pointed out that EAT attenuation can better predict obstructive CAD and high-risk plaque features than volume (32). Our findings provided further support for the existence of pan-heart inflammation and ongoing inflammatory risk in the post-AMI group.

Our analysis also identified a positive correlation between CCTA-derived PVAT mean attenuation and NCCT-derived EAT mean attenuation, supporting the use of NCCT-derived EAT mean attenuation as a PVAT attenuation surrogate. NCCT is more cost-effective and accessible than CCTA and does not involve the use of iodinated contrast agents, which can affect fat attenuation measurements and limit the usage in patients with compromised renal function (5, 29). Furthermore, EAT provides a more comprehensive measure of inflammation across the entire heart, as opposed to PVAT around selected vessel segments. EAT's ability to reflect pan-cardiac inflammation avoids the sampling errors associated with PVAT's localized measurements. Therefore, NCCT-derived EAT mean attenuation could provide a reliable and affordable surrogate for CCTA-derived PVAT measurements.

Our results align with existing research that points to adipose tissue's inflammatory role in cardiovascular disease. Previous research suggests that 30 to 60% of patients post-AMI treatment retain residual inflammatory risk (33, 34). This significant level of risk proposes a strong case for incorporating PVAT and EAT measurements into regular post-AMI evaluations. Furthermore, our study introduces the -70 HU as a potential threshold that may indicate EAT inflammation, offering a tangible measure that could enhance patient risk assessment and inform treatment approaches. Although our findings do not align with the Eisenberg et al. from the

EISNER trial that correlated decreased EAT attenuation with major adverse cardiac events (MACE) risk (10), this discrepancy may be due to several differences in study design and patient populations. First, we examined post-AMI patients who underwent imaging within 2 months after AMI incidence, whereas the EISNER trial scanned asymptomatic subjects approximately 14 years before MACE. Also, in the EISNER trial, most MACE events were late revascularizations, with only 19% representing AMI, while all our patients had experienced AMI before scanning. These differences suggest that there may be specific changes in EAT attenuation occurring near the time of an AMI, warranting further investigation into the temporal dynamics of EAT inflammation.

Future studies should explore longitudinal changes in PVAT and EAT inflammation, especially after medical interventions, to understand how treatments affect these inflammatory markers. While our findings are clinically significant for identifying ongoing inflammation in post-AMI patients, they may also have the potential to identify patients at risk of developing AMI who may benefit from intensified preventive care. Clinical trials have shown that metabolic drugs like glucagon-like peptide 1 receptor agonists and sodium-glucose co-transporter 2 inhibitors can decrease major cardiovascular events, likely by reducing EAT inflammation and altering its metabolism. These medications were shown to reduce EAT volume and thickness, but their effect on EAT attenuation is still unclear (5). Research should also include a wider range of patients to confirm the generalizability of our results. Exploring the biological mechanisms behind PVAT and EAT inflammation may also lead to new treatments for managing inflammation in cardiovascular disease.

Limitations

There are some limitations to this study. First, this study is observational and may be susceptible to unmeasured confounding factors and referral bias, and the use of propensity-matching could introduce additional biases. Second, although we attempted to control for major confounders,

differences in BMI and hyperlipidemia between the matched cohorts could still introduce bias in EAT and PVAT measurements. To address this, we conducted sensitivity analyses with a smaller BMI-matched cohort and with only Chinese subjects. However, these factors remain a potential source of residual confounding, especially for under-represented non-Chinese patients. Third, due to CCTA's limitations in analyzing areas adjacent to high-density materials, we excluded stented vessels from the analysis, potentially leading to an underestimation of the inflammatory state in post-AMI patients. Additionally, while calcification is a known marker of AMI and subsequent cardiac events, heavy calcification can interfere with the precise CT measurement of perivascular tissue. We acknowledge that calcification may influence HU measurements of surrounding tissue, especially for EAT, but we cannot distinguish this effect from underlying biological changes in inflammation. Fourth, due to the inherent limitation of CT, we cannot differentiate adipose tissue attenuation change caused by inflammation from other causes, such as post-AMI edema. Fifth, the male-dominant study population may limit the generalizability of our findings. Although females were approached in equal proportion for consent, a large majority opted out of the post-AMI arm due to personal preferences. Sixth, due to the multicenter nature of our study, we could not standardize the usage of the iodinated contrast throughout all CCTA scans, which may introduce variations in PVAT attenuation measurement. Finally, as we do not have longitudinal follow-up of these patients, we cannot be certain whether the high PVAT and EAT attenuation in post-AMI patients is temporal or chronic.

Conclusion

Our study reveals that post-AMI patients exhibit significantly increased PVAT and EAT mean attenuation compared to those with stable CAD, pointing out a possibility of CT-quantifying residual inflammatory response. Furthermore, there is a correlation between PVAT and EAT quantification, facilitating the use of NCCT as an affordable, non-contrast surrogate for PVAT

measurements. Our results also show that EAT volume percentage above the -70 HU threshold is a potential marker of EAT inflammation. These findings propose a novel approach to evaluate residual inflammation in post-treatment AMI patients.

Supplementary Data

- Supplementary Method
- Supplementary Result of Sensitivity Analyses
- Supplementary Figure S1, S2
- Supplementary Table S1 – S8

Acknowledgments

DJH is supported by the Duke-NUS Signature Research Programme funded by the Ministry of Health, Singapore Ministry of Health's National Medical Research Council under its Singapore Translational Research Investigator Award (MOH-STaR21jun-0003), Centre Grant scheme (NMRC CG21APR1006), and Collaborative Centre Grant scheme (NMRC/CG21APRC006). LB is supported by the Singapore Ministry of Health National Medical Research Council's Transition Award (MOH-001145-00). LZ is supported by Industry Alignment Fund Pre Position by the A*STAR, National Research Foundation and EDB (H20c6a0035) and Singapore Ministry of Health's National Medical Research Council under its Health Service Grant (MOH-000358). CHS was supported by the National University of Singapore Yong Loo Lin School of Medicine's Junior Academic Fellowship Scheme, as well as the Singapore Ministry of Health National Medical Research Council's Transition Award (MOH-001368-00).

Disclosure

LJS sits on the International Editorial Board of the European Heart Journal – Cardiovascular Imaging. Other authors have no conflict of interest to declare.

Data Availability Statement

The data underlying this article will be shared on reasonable request to the corresponding author.

Reference

1. Libby P, Buring JE, Badimon L, Hansson GK, Deanfield J, Bittencourt MS, et al. Atherosclerosis. Nat Rev Dis Primers. 2019;5(1):56.
2. Cassar A, Holmes DR, Jr., Rihal CS, Gersh BJ. Chronic coronary artery disease: diagnosis and management. Mayo Clin Proc. 2009;84(12):1130-46.
3. Ralapanawa U, Sivakanesan R. Epidemiology and the Magnitude of Coronary Artery Disease and Acute Coronary Syndrome: A Narrative Review. J Epidemiol Glob Health. 2021;11(2):169-77.
4. Antoniades C, Kotanidis CP, Berman DS. State-of-the-art review article. Atherosclerosis affecting fat: What can we learn by imaging perivascular adipose tissue? J Cardiovasc Comput Tomogr. 2019;13(5):288-96.
5. Iacobellis G. Epicardial adipose tissue in contemporary cardiology. Nat Rev Cardiol. 2022;19(9):593-606.
6. Antoniades C, Antonopoulos AS, Deanfield J. Imaging residual inflammatory cardiovascular risk. Eur Heart J. 2020;41(6):748-58.
7. Lee SE, Sung JM, Andreini D, Al-Mallah MH, Budoff MJ, Cademartiri F, et al. Association Between Changes in Perivascular Adipose Tissue Density and Plaque Progression. JACC Cardiovasc Imaging. 2022;15(10):1760-7.
8. Oikonomou EK, Antoniades C. The role of adipose tissue in cardiovascular health and disease. Nat Rev Cardiol. 2019;16(2):83-99.
9. Tarsitano MG, Pandozzi C, Muscogiuri G, Sironi S, Pujia A, Lenzi A, et al. Epicardial Adipose Tissue: A Novel Potential Imaging Marker of Comorbidities Caused by Chronic Inflammation. Nutrients. 2022;14(14).
10. Eisenberg E, McElhinney PA, Commandeur F, Chen X, Cadet S, Goeller M, et al. Deep Learning-Based Quantification of Epicardial Adipose Tissue Volume and Attenuation Predicts Major Adverse Cardiovascular Events in Asymptomatic Subjects. Circ Cardiovasc Imaging. 2020;13(2):e009829.
11. Dai X, Yu L, Lu Z, Shen C, Tao X, Zhang J. Serial change of perivascular fat attenuation index after statin treatment: Insights from a coronary CT angiography follow-up study. Int J Cardiol. 2020;319:144-9.
12. Ouwens DM, Sell H, Greulich S, Eckel J. The role of epicardial and perivascular adipose tissue in the pathophysiology of cardiovascular disease. J Cell Mol Med. 2010;14(9):2223-34.
13. Tanaka K, Sata M. Roles of Perivascular Adipose Tissue in the Pathogenesis of Atherosclerosis. Front Physiol. 2018;9:3.
14. Thygesen K, Alpert JS, Jaffe AS, Chaitman BR, Bax JJ, Morrow DA, et al. Fourth Universal Definition of Myocardial Infarction (2018). J Am Coll Cardiol. 2018;72(18):2231-64.
15. Ho D, Imai K, King G, Stuart EA. MatchIt: Nonparametric Preprocessing for Parametric Causal Inference. Journal of Statistical Software. 2011;42(8):1 - 28.
16. Leipsic J, Abbara S, Achenbach S, Cury R, Earls JP, Mancini GJ, et al. SCCT guidelines for the interpretation and reporting of coronary CT angiography: a report of the Society of Cardiovascular Computed Tomography Guidelines Committee. J Cardiovasc Comput Tomogr. 2014;8(5):342-58.
17. Abbara S, Blanke P, Maroules CD, Cheezum M, Choi AD, Han BK, et al. SCCT guidelines for the performance and acquisition of coronary computed tomographic angiography: A report of the society of Cardiovascular Computed Tomography Guidelines Committee: Endorsed by the North American Society for Cardiovascular Imaging (NASCI). J Cardiovasc Comput Tomogr. 2016;10(6):435-49.
18. Park HB, Lee BK, Shin S, Heo R, Arsanjani R, Kitslaar PH, et al. Clinical Feasibility of 3D Automated Coronary Atherosclerotic Plaque Quantification Algorithm on Coronary Computed Tomography Angiography: Comparison with Intravascular Ultrasound. Eur Radiol. 2015;25(10):3073-83.

19. Antonopoulos AS, Sanna F, Sabharwal N, Thomas S, Oikonomou EK, Herdman L, et al. Detecting human coronary inflammation by imaging perivascular fat. Sci Transl Med. 2017;9(398).
20. Oikonomou EK, Marwan M, Desai MY, Mancio J, Alashi A, Hutt Centeno E, et al. Non-invasive detection of coronary inflammation using computed tomography and prediction of residual cardiovascular risk (the CRISP CT study): a post-hoc analysis of prospective outcome data. Lancet. 2018;392(10151):929-39.
21. Goeller M, Tamarappoo BK, Kwan AC, Cadet S, Commandeur F, Razipour A, et al. Relationship between changes in pericoronary adipose tissue attenuation and coronary plaque burden quantified from coronary computed tomography angiography. Eur Heart J Cardiovasc Imaging. 2019;20(6):636-43.
22. Nomura CH, Assuncao-Jr AN, Guimarães PO, Liberato G, Morais TC, Fahel MG, et al. Association between perivascular inflammation and downstream myocardial perfusion in patients with suspected coronary artery disease. Eur Heart J Cardiovasc Imaging. 2020;21(6):599-605.
23. Kikinis R, Pieper SD, Vosburgh KG. 3D Slicer: A Platform for Subject-Specific Image Analysis, Visualization, and Clinical Support. In: Jolesz FA, editor. Intraoperative Imaging and Image-Guided Therapy. New York, NY: Springer New York; 2014. p. 277-89.
24. Commandeur F, Goeller M, Razipour A, Cadet S, Hell MM, Kwiecinski J, et al. Fully Automated CT Quantification of Epicardial Adipose Tissue by Deep Learning: A Multicenter Study. Radiol Artif Intell. 2019;1(6):e190045.
25. Chang HJ, Lin FY, Lee SE, Andreini D, Bax J, Cademartiri F, et al. Coronary Atherosclerotic Precursors of Acute Coronary Syndromes. J Am Coll Cardiol. 2018;71(22):2511-22.
26. Mancio J, Azevedo D, Saraiva F, Azevedo AI, Pires-Morais G, Leite-Moreira A, et al. Epicardial adipose tissue volume assessed by computed tomography and coronary artery disease: a systematic review and meta-analysis. Eur Heart J Cardiovasc Imaging. 2018;19(5):490-7.
27. Lu MT, Park J, Ghemigian K, Mayrhofer T, Puchner SB, Liu T, et al. Epicardial and paracardial adipose tissue volume and attenuation - Association with high-risk coronary plaque on computed tomographic angiography in the ROMICAT II trial. Atherosclerosis. 2016;251:47-54.
28. Mahabadi AA, Balcer B, Dykun I, Forsting M, Schlosser T, Heusch G, et al. Cardiac computed tomography-derived epicardial fat volume and attenuation independently distinguish patients with and without myocardial infarction. PLoS One. 2017;12(8):e0183514.
29. Liu Z, Wang S, Wang Y, Zhou N, Shu J, Stamm C, et al. Association of epicardial adipose tissue attenuation with coronary atherosclerosis in patients with a high risk of coronary artery disease. Atherosclerosis. 2019;284:230-6.
30. Franssens BT, Nathoe HM, Leiner T, van der Graaf Y, Visseren FL. Relation between cardiovascular disease risk factors and epicardial adipose tissue density on cardiac computed tomography in patients at high risk of cardiovascular events. Eur J Prev Cardiol. 2017;24(6):660-70.
31. Iacobellis G, Secchi F, Capitanio G, Basilico S, Schiaffino S, Boveri S, et al. Epicardial Fat Inflammation in Severe COVID-19. Obesity (Silver Spring). 2020;28(12):2260-2.
32. Pandey NN, Sharma S, Jagia P, Kumar S. Epicardial fat attenuation, not volume, predicts obstructive coronary artery disease and high risk plaque features in patients with atypical chest pain. Br J Radiol. 2020;93(1114):20200540.
33. Ridker PM. Clinician's Guide to Reducing Inflammation to Reduce Atherothrombotic Risk: JACC Review Topic of the Week. J Am Coll Cardiol. 2018;72(25):3320-31.
34. Ridker PM. How Common Is Residual Inflammatory Risk? Circ Res. 2017;120(4):617-9.

Legends

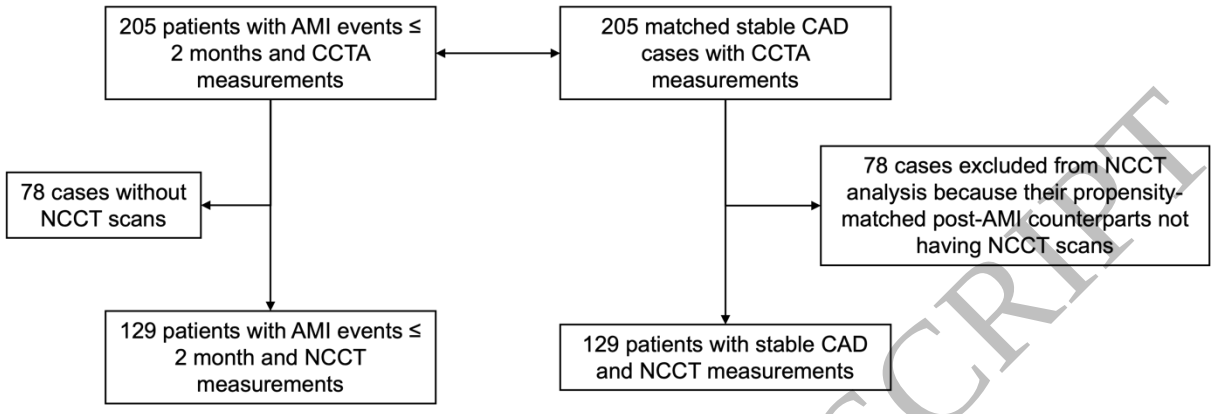

Figure 1. CONSORT diagram for the study. *(AMI: acute myocardial infarction, CAD: coronary artery disease, CCTA: coronary computed tomography angiography, NCCT: non-contrast computed tomography).*

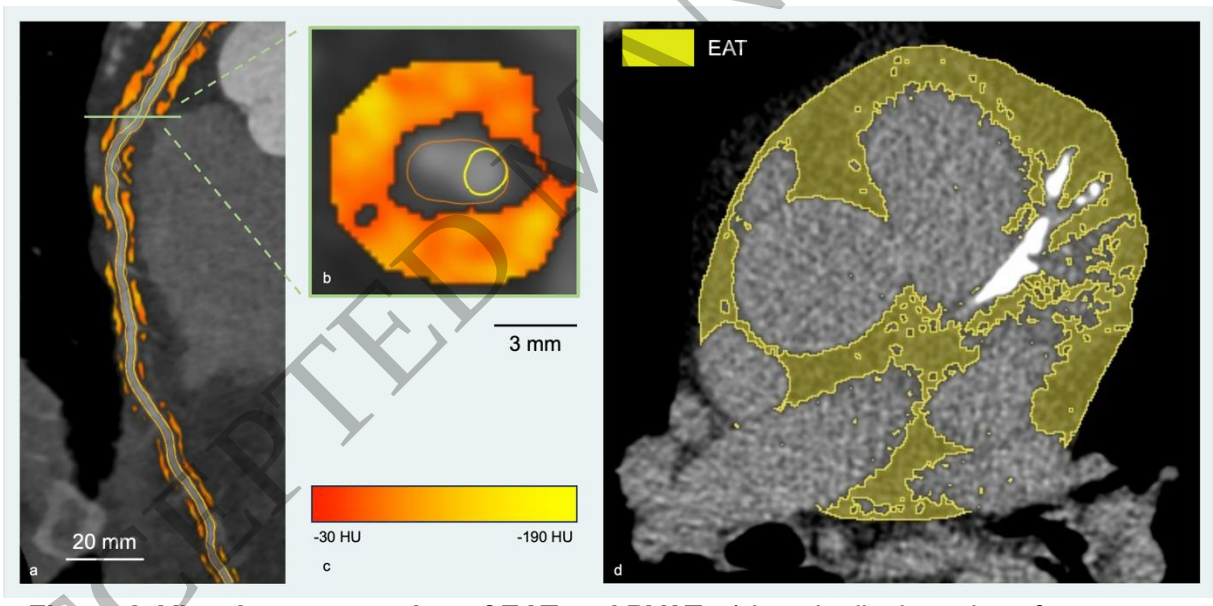

Figure 2. Visual representation of EAT and PVAT. a) Longitudinal section of a coronary vessel with PVAT; b) a cross-section of a coronary plaque PVAT in CCTA scan (at the green bar level of [a]); c) a color diagram of PVAT attenuation; d) EAT in NCCT scan (EAT is colored in yellow). (CCTA: coronary computed tomography angiography, EAT: epicardial adipose tissue, NCCT: non-contrast computed tomography; PVAT: perivascular adipose tissue)

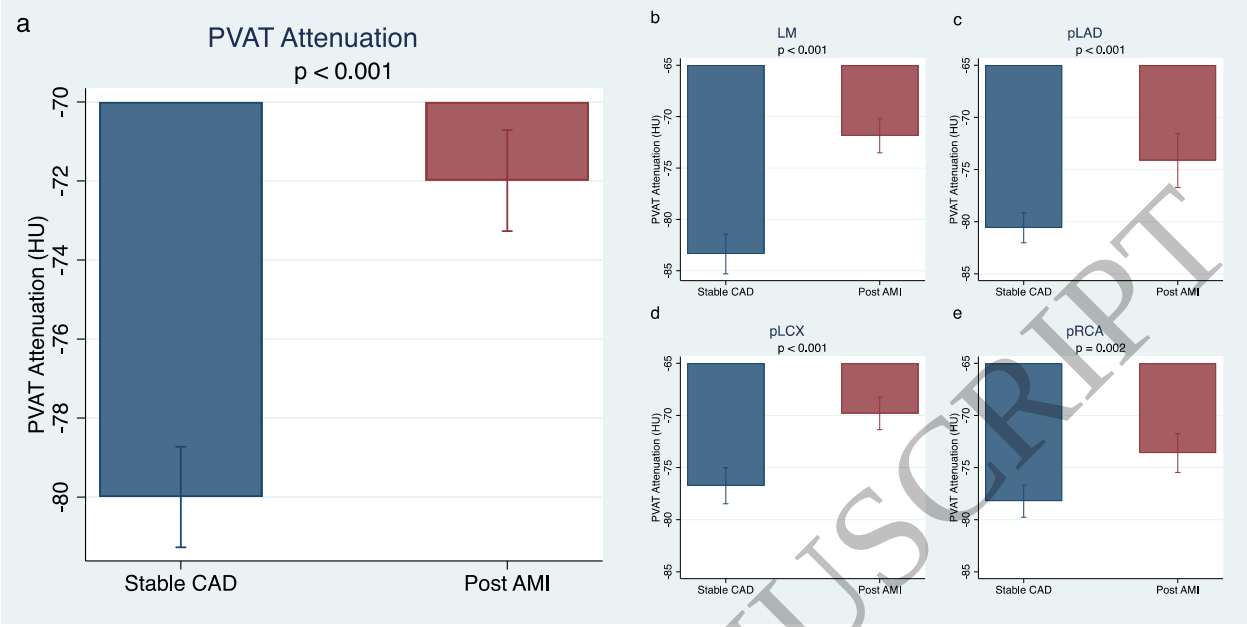

Figure 3. The regression model predicted PVAT mean attenuation for post-AMI (excluding culprit vessels) and stable CAD patients after averaging covariates. a) total PVAT mean attenuation; b) left main coronary artery (LM); c) proximal left anterior descending coronary artery (pLAD); d) proximal left circumflex coronary artery (pLCX); e) proximal right coronary artery (pRCA).

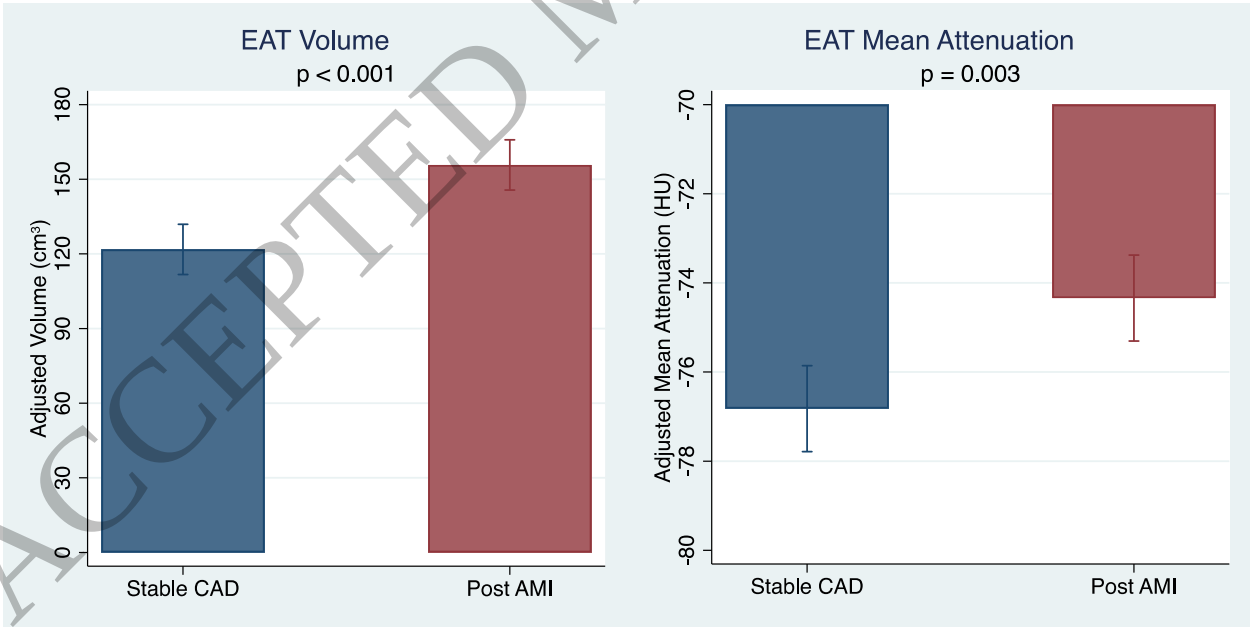

Figure 4. The regression model predicted EAT characteristics for post-AMI and stable CAD patients after averaging covariates. (left) EAT volume; (right) EAT mean attenuation (EAT: epicardial adipose tissue).

Table 1. Clinical characteristics of post-AMI and stable CAD patients.

Variables	CCTA Cases			NCCT Cases		
	Post AMI	Stable CAD	P-value	Post AMI	Stable CAD	P-value
	(n= 205)	(n= 205)		(n= 129)	(n= 129)	
	N (%) or Mean ± SD			N (%) or Mean ± SD		
Age, year	59.8 ± 9.2	60.5 ± 10.0	0.431	60.7 ± 8.9	61.0 ± 9.4	0.807
Male, %	189 (92.20)	185 (90.24)	0.485	117 (90.70)	114 (88.37)	0.542
Risk factors						
Hypertension, %	94 (45.85)	102 (49.76)	0.429	57 (44.19)	70 (54.26)	0.105
Hyperlipidemia, %	102 (49.76)	119 (58.05)	0.092	54 (41.86)	78 (60.47)	0.003
Lipid Control Medication, %	101 (49.27)	124 (60.49)	0.022	28 (21.71)	21 (16.28)	0.267
Diabetes, %	42 (20.49)	38 (18.54)	0.618	22 (17.05)	26 (20.16)	0.522
Smoking (current, %)	48 (23.41)	53 (25.85)	0.816	28 (21.71)	21 (16.28)	0.267
Premature family history CAD, %	49 (23.90)	47 (22.93)	0.567	39 (30.23)	38 (29.46)	0.892
Propensity Score	0.426 ± 0.182	0.396 ± 0.182	0.105	0.430 ± 0.169	0.447 ± 0.113	0.355
Race/Ethnicity			< 0.05			< 0.05
Not known	6 (2.93)	3 (1.46)		2 (1.55)	2 (1.55)	
Chinese	94 (45.85)	157 (76.59)		45 (34.88)	102 (79.07)	
Indian	29 (14.15)	19 (9.27)		15 (11.63)	8 (6.2)	
Malay	18 (8.78)	8 (3.90)		11 (8.53)	5 (3.88)	
Caucasian	54 (26.34)	2 (0.98)		54 (41.86)	2 (1.55)	
Other	4 (1.95)	16 (7.80)		2 (1.55)	10 (7.75)	
Body Mass Index, kg/m^2	27.3 ± 4.5	25.8 ± 5.2	0.001	27.9 ± 4.5	26.1 ± 5.9	0.005

AMI: acute myocardial infarction, CAD: coronary artery disease; CCTA: coronary computed tomography angiography; NCCT: non-contrast computed tomography.

Table 2. The multivariate regression coefficients of PVAT and EAT characteristics of the post-AMI group (stable CAD as baseline).

Outcome	Estimate	Standard error	P value	[95% confidence interval]	
PVAT mean attenuation (HU)*					
Pooled†	8.01	1.07	< 0.001	5.90	10.11
LM†	11.50	1.48	< 0.001	8.59	14.41
pLAD†	6.45	1.75	< 0.001	3.02	9.89
pLCX†	6.93	1.37	< 0.001	4.22	9.63
pRCA†	4.62	1.45	0.002	1.76	7.48
EAT Characteristics					
EAT Mean Attenuation (HU)‡	2.48	0.84	0.003	0.83	4.13
EAT Volume (cm^3)§	33.93	8.66	< 0.001	16.86	51.00

* Vessel segments of culprit vessels were excluded

† Models adjusted for age, gender, race, disease history (hypertension, diabetes, and hyperlipidemia), family CAD history, smoking status, use of lipid control, BMI, CT tube voltage, and lumen attenuation

‡ Models adjusted for age, gender, race, disease history (hypertension, diabetes, and hyperlipidemia), family CAD history, smoking status, use of lipid control, BMI, CT tube voltage, and EAT volume

§ Models adjusted for age, gender, race, disease history (hypertension, diabetes, and hyperlipidemia), family CAD history, smoking status, use of lipid control, BMI, and CT scan tube voltage

AMI: acute myocardial infarction, BMI: body mass index; CAD: coronary artery disease; EAT: epicardial adipose tissue; LM: left main; PVAT: perivascular adipose tissue; pLAD: proximal left anterior descending artery; pLCX: proximal left circumflex artery; pRCA: proximal right coronary artery.

Table 3. Clinical characteristics of post-AMI and stable CAD patients.

Variables	CCTA Cases			NCCT Cases		
	Post AMI (n= 205)	Stable CAD (n= 205)	P-value	Post AMI (n= 129)	Stable CAD (n= 129)	P-value
	N (%) or Mean ± SD			N (%) or Mean ± SD		
Age, year	59.8 ± 9.2	60.5 ± 10.0	0.431	60.7 ± 8.9	61.0 ± 9.4	0.807
Male, %	189 (92.20)	185 (90.24)	0.485	117 (90.70)	114 (88.37)	0.542
Risk factors						
Hypertension, %	94 (45.85)	102 (49.76)	0.429	57 (44.19)	70 (54.26)	0.105
Hyperlipidemia, %	102 (49.76)	119 (58.05)	0.092	54 (41.86)	78 (60.47)	0.003
Lipid Control Medication, %	101 (49.27)	124 (60.49)	0.022	28 (21.71)	21 (16.28)	0.267
Diabetes, %	42 (20.49)	38 (18.54)	0.618	22 (17.05)	26 (20.16)	0.522
Smoking (current, %)	48 (23.41)	53 (25.85)	0.816	28 (21.71)	21 (16.28)	0.267
Premature family history CAD, %	49 (23.90)	47 (22.93)	0.567	39 (30.23)	38 (29.46)	0.892
Propensity Score	0.426 ± 0.182	0.396 ± 0.182	0.105	0.430 ± 0.169	0.447 ± 0.113	0.355
Race/Ethnicity			< 0.05			< 0.05
Not known	6 (2.93)	3 (1.46)		2 (1.55)	2 (1.55)	
Chinese	94 (45.85)	157 (76.59)		45 (34.88)	102 (79.07)	
Indian	29 (14.15)	19 (9.27)		15 (11.63)	8 (6.2)	
Malay	18 (8.78)	8 (3.90)		11 (8.53)	5 (3.88)	
Caucasian	54 (26.34)	2 (0.98)		54 (41.86)	2 (1.55)	

Other	4 (1.95)	16 (7.80)		2 (1.55)	10 (7.75)	
Body Mass Index, kg/m^2	27.3 ± 4.5	25.8 ± 5.2	0.001	27.9 ± 4.5	26.1 ± 5.9	0.005

AMI: acute myocardial infarction, CAD: coronary artery disease; CCTA: coronary computed tomography angiography; NCCT: non-contrast computed tomography.

Table 4. The multivariate regression coefficients of PVAT and EAT characteristics of the post-AMI group (stable CAD as baseline).

Outcome	Estimate	Standard error	P value	[95% confidence interval]	
PVAT mean attenuation (HU)*					
Pooled†	8.01	1.07	< 0.001	5.90	10.11
LM†	11.50	1.48	< 0.001	8.59	14.41
pLAD†	6.45	1.75	< 0.001	3.02	9.89
pLCX†	6.93	1.37	< 0.001	4.22	9.63
pRCA†	4.62	1.45	0.002	1.76	7.48
EAT Characteristics					
EAT Mean Attenuation (HU)‡	2.48	0.84	0.003	0.83	4.13
EAT Volume (cm^3)§	33.93	8.66	< 0.001	16.86	51.00

* Vessel segments of culprit vessels were excluded

† Models adjusted for age, gender, race, disease history (hypertension, diabetes, and hyperlipidemia), family CAD history, smoking status, use of lipid control, BMI, CT tube voltage, and lumen attenuation

‡ Models adjusted for age, gender, race, disease history (hypertension, diabetes, and hyperlipidemia), family CAD history, smoking status, use of lipid control, BMI, CT tube voltage, and EAT volume

§ Models adjusted for age, gender, race, disease history (hypertension, diabetes, and hyperlipidemia), family CAD history, smoking status, use of lipid control, BMI, and CT scan tube voltage

AMI: acute myocardial infarction, BMI: body mass index; CAD: coronary artery disease; EAT: epicardial adipose tissue; LM: left main; PVAT: perivascular adipose tissue; pLAD: proximal left anterior descending artery; pLCX: proximal left circumflex artery; pRCA: proximal right coronary artery.

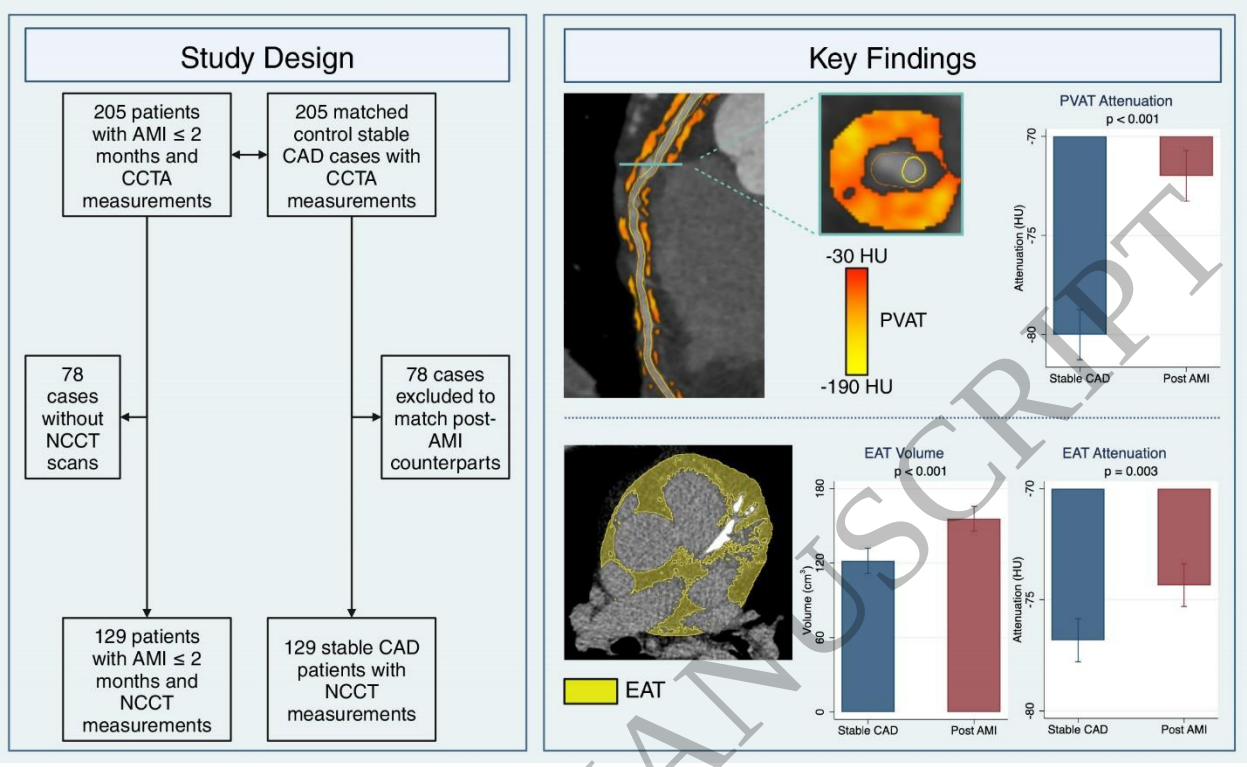

Graphical Abstract